Electronic Supplementary Material (ESI) for Journal of Materials Chemistry C.

Supporting materials

CdS/Sb_2S_3 heterojunction thin film solar cells with thermally-evaporated absorber

Xu Chen[a], Zhiqiang Li[a *], Hongbing Zhu[a], Ying Wang[a], Baolai Liang[a], Jingwei Chen[a], Ying Xu[a], Yaohua Mai[a,b *]

[a]*College of Physics Science and Technology, Hebei University, Baoding 071002, China*

[b]*Institute of New Energy Technology, Jinan University, Guangzhou 510632, China*

[*] Corresponding author.

Email: lizhiqiang@hbu.edu.cn (Zhiqiang Li), yaohuamai@jnu.edu.cn (Yaohua Mai).

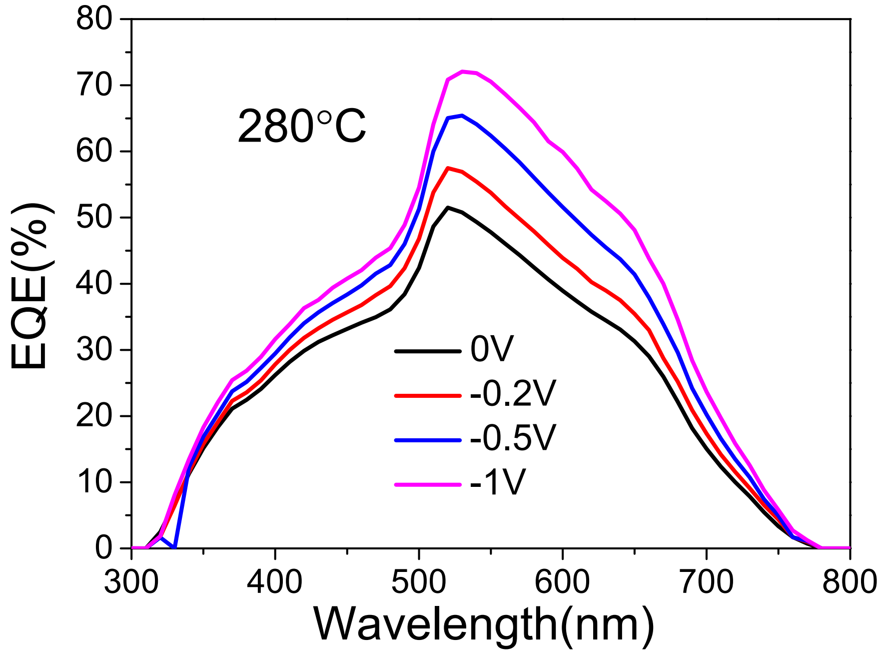

Fig.S1 EQE spectra at different voltage bias of solar cells with Sb_2S_3 absorber layer deposited at 280 °C.

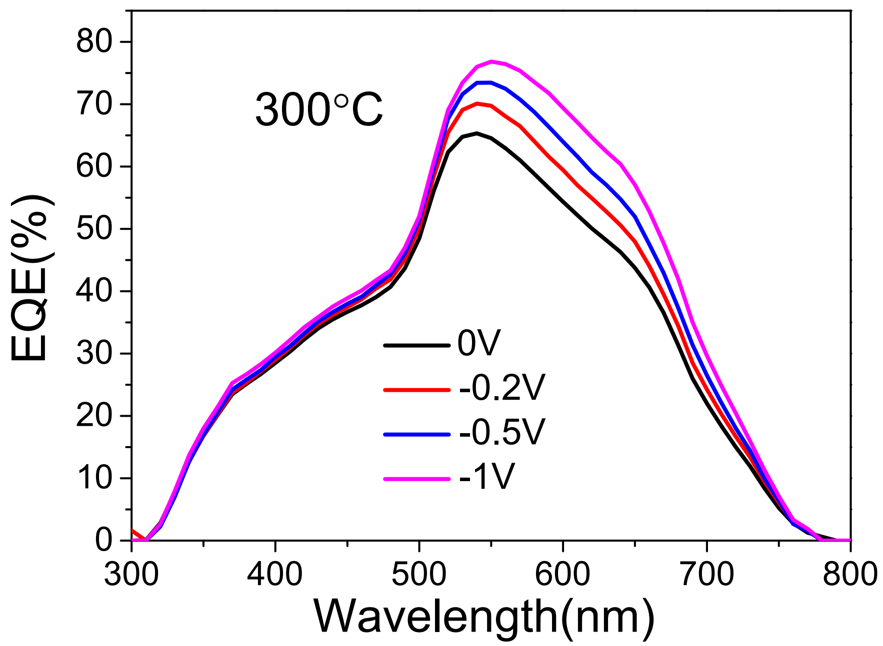

Fig.S2 EQE spectra at different voltage bias of solar cells with Sb_2S_3 absorber layer deposited at 300 °C.

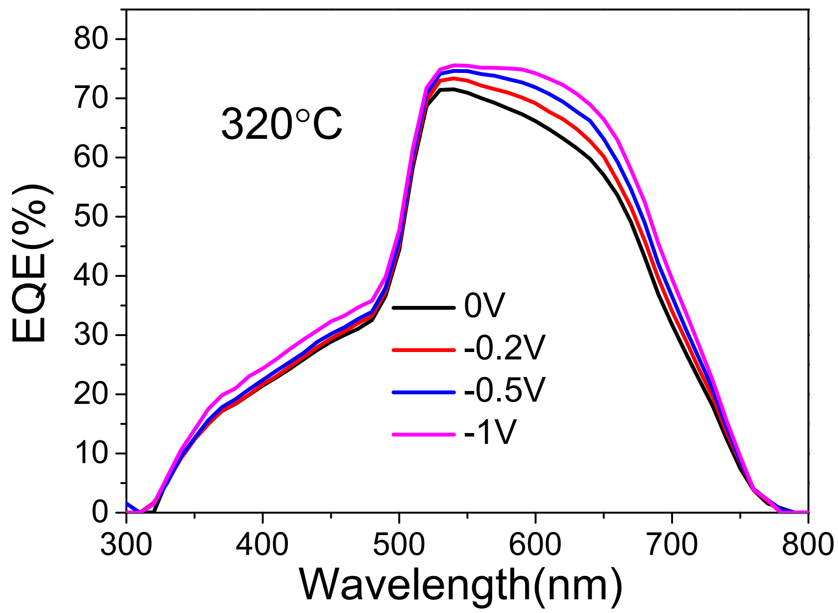

Fig.S3 EQE spectra at different voltage bias of solar cells with Sb_2S_3 absorber layer deposited at 320 °C.

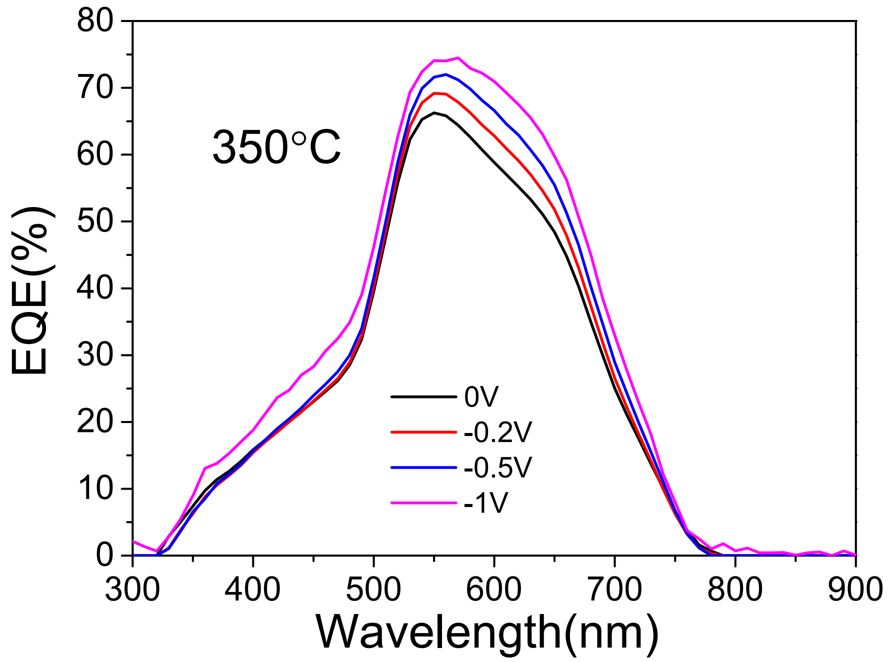

Fig.S4 EQE spectra at different voltage bias of solar cells with Sb_2S_3 absorber layer deposited at 350 °C.

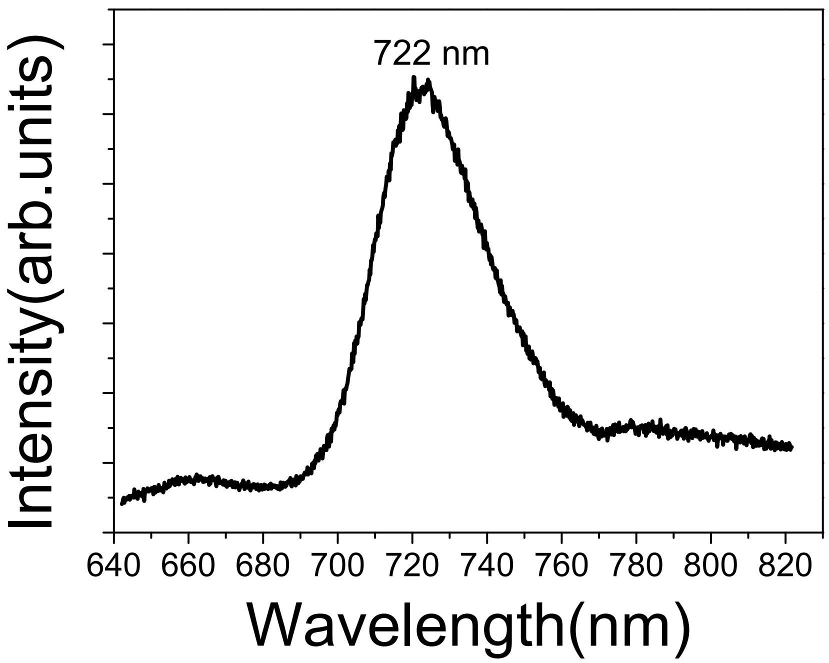

Fig.S5 PL spectrum of Sb_2S_3 thin films, excited by laser of 470 nm at 77 K.

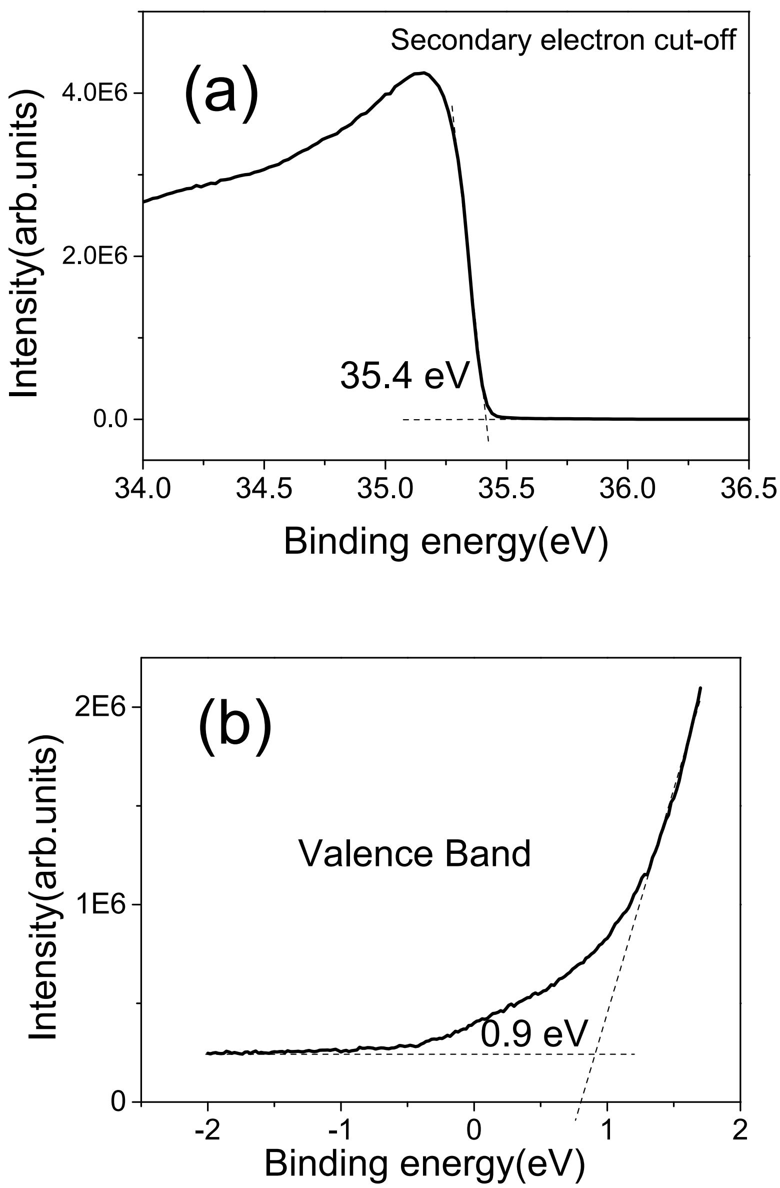

Fig.S6 The UPS spectra at (a) cutoff region, and (b) valence band region of Sb_2S_3 thin films. The valence-band spectra were measured with a photon energy of 40 eV and referenced to the Fermi level ($E_F = 0$). A sample bias of −5 V was applied to observe the secondary electron cutoff. The work function (ϕ) is determined by the difference between the photon energy and the binding energy of the secondary cutoff edge.

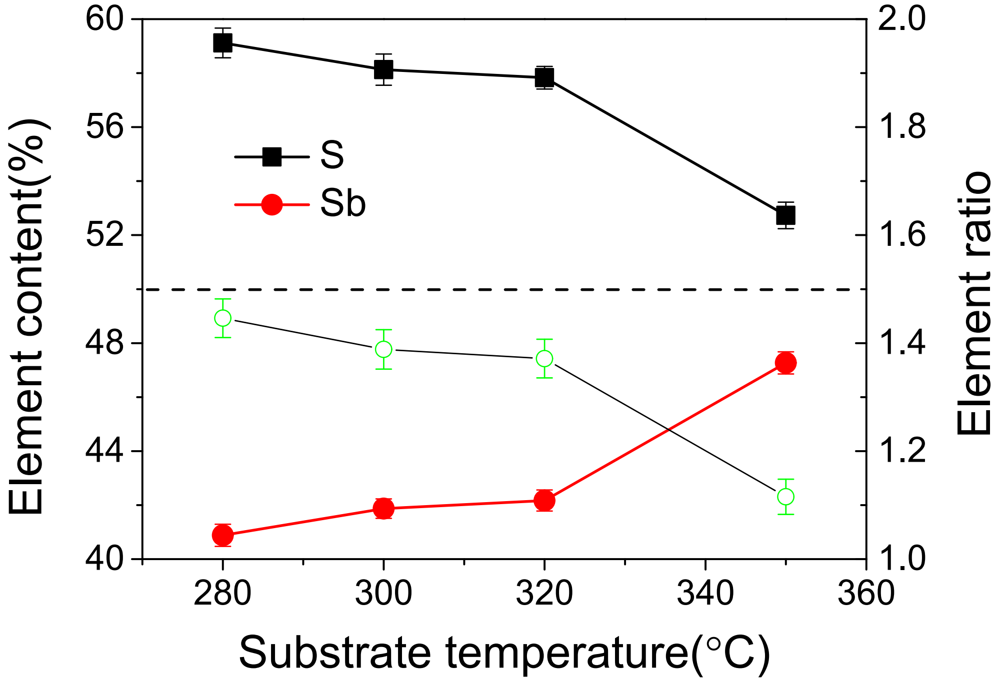

Fig.S7 EDX analysis of the Sb_2S_3 films deposited on bare glass substrates. The solid square and solid circle are atomic percent of antimony and sulfur, respectively. The hollow circle is element ratios. All of the samples exhibited sulfur deficiency, and this behavior became more serious as the growth temperature increased from 280°C to 350°C. The S/Sb ratio was about 1.12 for the sample deposited at 350°C and the S loss was about 25%.

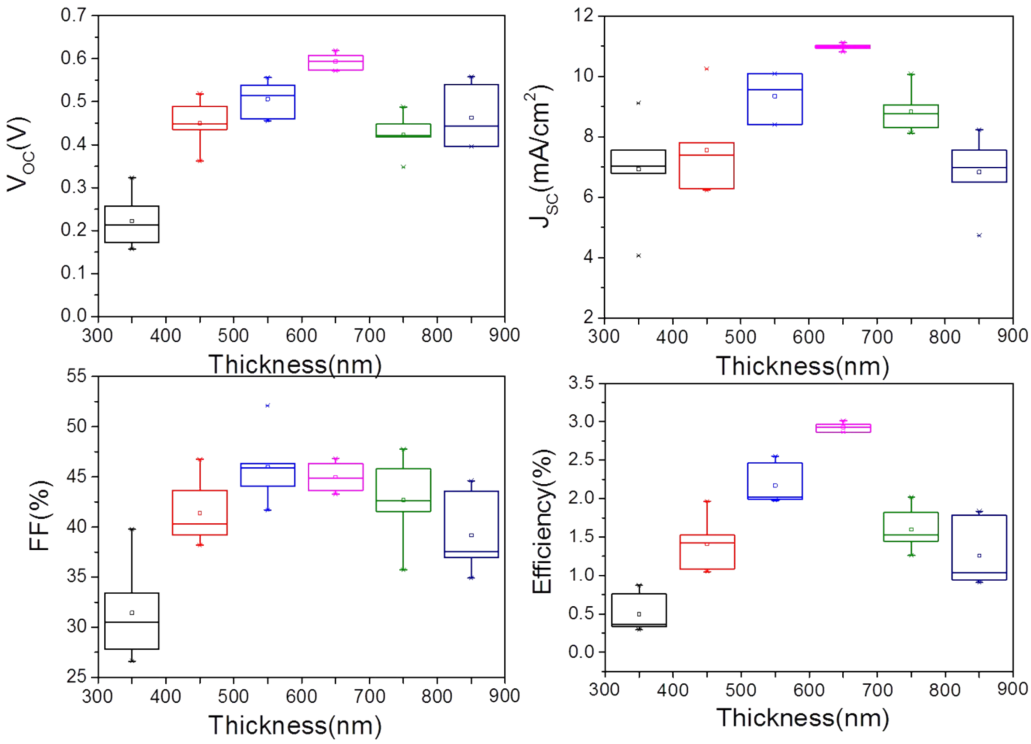

Fig.S8 Photovoltaic performances as a function of Sb_2S_3 absorber thickness.

Table S1 Summary of Sb_2S_3-based solar cells with efficiencies higher than 5%. Note that ds was short for dense and mp was short for mesoscopic, respectively.

<table>
<tr><th colspan="2">Device configuration</th><th>Eff. (%)</th><th>Voc (mV)</th><th>Jsc (mA/cm^2)</th><th>FF (%)</th><th>Ref.</th></tr>
<tr><td rowspan="6">Mesoscopic Sb_2S_3-sensitized solar cells</td><td>FTO/ds-TiO_2/mp-TiO2/Sb_2S_3/Spiro-MeoTAD/Au</td><td>5.2 (10% sun)</td><td>545</td><td>1.51 (10% sun)</td><td>64</td><td>[1]</td></tr>
<tr><td>FTO/ds-TiO2/mp-TiO_2/Sb_2S_3/PCPDTBT/Au</td><td>7.5</td><td>711</td><td>16.1</td><td>65</td><td>[2]</td></tr>
<tr><td>FTO/ds-TiO_2/mp-TiO_2/Sb_2S_3/ PCPDTBT(P3HT) /PEDOT:PSS /Au</td><td>6.4</td><td>596</td><td>16.1</td><td>67</td><td>[3]</td></tr>
<tr><td>FTO/ds-TiO2/mp-TiO2/Sb_2S_3/PCPDTBT PCBM/PEDOT:PSS/Au</td><td>5.1</td><td>548</td><td>13.9</td><td>67.7</td><td>[4]</td></tr>
<tr><td>FTO/ds-TiO2/BaTio3/MgO/Sb2S3/CuSCN/Au</td><td>5.7</td><td>607</td><td>16.5</td><td>57.2</td><td>[5]</td></tr>
<tr><td>FTO//ds-TiO2/mp-TiO2/Sb_2S_3/PCPDTBT/Au</td><td>6.2</td><td>616</td><td>15.3</td><td>65.7</td><td>[6]</td></tr>
<tr><td rowspan="2">Planar heterojunction</td><td>FTO/TiO_2/Sb_2S_3/P3HT/Au</td><td>5.77</td><td>670</td><td>14.92</td><td>58.04</td><td>[7]</td></tr>
<tr><td>FTO/TiO2/ $Sb_2(S,Se)_3$/Spiro-OMeDAT/Au</td><td>5.71</td><td>560</td><td>19.48</td><td>52.7</td><td>[8]</td></tr>
</table>

Reference:

[1] S.-J. Moon, Y. Itzhaik, J.-H. Yum, S.M. Zakeeruddin, G. Hodes, M. Grätzel, Sb_2S_3-Based Mesoscopic Solar Cell using an Organic Hole Conductor, The Journal of Physical Chemistry Letters, 1 (2010) 1524-1527.

[2] Y. C. Choi, D.U. Lee, J.H. Noh, E.K. Kim, S.I. Seok, Highly Improved Sb_2S_3 sensitized-inorganic-organic heterojunction solar cells and quantification of traps by deep-level transient spectroscopy, Adv. Funct. Mater., 24 (2014) 3587-3592.

[3] Y. C. Choi, S. I. Seok, Efficient Sb_2S_3-sensitized solar cells via single-step deposition of Sb_2S_3 using S/Sb ratio controlled $SbCl_3$-thiourea complex solution, Adv. Funct. Mater., 25 (2015) 2892-2898.

[4] K.C. GoDel, Y.C. Choi, B. Roose, A. Sadhanala, H.J. Snaith, S.I. Seok, U. Steiner, S.K. Pathak, Efficient room temperature aqueous Sb_2S_3 synthesis for inorganic-organic sensitized solar cells with 5.1% efficiencies, Chem. Comm., 51 (2015) 8640.

[5] S. Ito, K. Tsujimoto, D.C. Nguyen, K. Manabe, H. Nishino, Doping effects in Sb_2S_3 absorber for full-inorganic printed solar cells with 5.7% conversion efficiency, Int. J. Hydrogen Energ., 38 (2013) 16749-16754.

[6] S.H. Im, C.-S. Lim, J.A. Chang, Y.H. Lee, N. Maiti, H.-J. Kim, M.K. Nazeeruddin, M. Grätzel, S.I. Seok, Toward interaction of sensitizer and functional moieties in hole-transporting materials for efficient semiconductor-sensitized solar cells, Nano Lett., 11 (2011) 4789-4793.

[7] D.-H. Kim, S.-J. Lee, M.S. Park, J.-K. Kang, J.H. Heo, S.H. Im, S.-J. Sung, Highly reproducible planar

Sb_2S_3-sensitized solar cells based on atomic layer deposition, Nanoscale, 6 (2014) 14549-14554.
[8] Y. Zhang, J. Li, G. Jiang, W. Liu, S. Yang, C. Zhu, T. Chen, Selenium-graded $Sb_2(S_{1-x}Se_x)_3$ for planar heterojunction solar cell delivering a certified power conversion efficiency of 5.71%, Solar RRL, 1 (2017) 1700017.